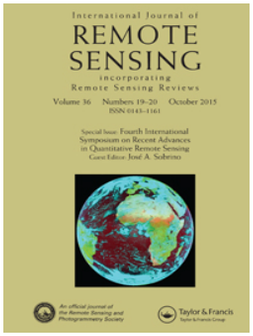

International Journal of Remote Sensing

ISSN: 0143-1161 (Print) 1366-5901 (Online) Journal homepage: http://www.tandfonline.com/loi/tres20

Global Atmospheric Profiles from Reanalysis Information (GAPRI): a new database for earth surface temperature retrieval

C. Mattar, C. Durán-Alarcón, J. C. Jiménez-Muñoz, A. Santamaría-Artigas, L. Olivera-Guerra & J. A. Sobrino

To cite this article: C. Mattar, C. Durán-Alarcón, J. C. Jiménez-Muñoz, A. Santamaría-Artigas, L. Olivera-Guerra & J. A. Sobrino (2015) Global Atmospheric Profiles from Reanalysis Information (GAPRI): a new database for earth surface temperature retrieval, International Journal of Remote Sensing, 36:19-20, 5045-5060, DOI: 10.1080/01431161.2015.1054965

To link to this article: http://dx.doi.org/10.1080/01431161.2015.1054965

Published online: 12 Jun 2015.

International Journal of Remote Sensing, 2015
Vol. 36, Nos. 19–20, 5045–5060, http://dx.doi.org/10.1080/01431161.2015.1054965

Taylor & Francis
Taylor & Francis Group

Global Atmospheric Profiles from Reanalysis Information (GAPRI): a new database for earth surface temperature retrieval

C. Mattar[a], C. Durán-Alarcón[a]*, J. C. Jiménez-Muñoz[b], A. Santamaría-Artigas[a], L. Olivera-Guerra[a], and J. A. Sobrino[b]

[a]*Laboratory for Analysis of the Biosphere (LAB), University of Chile, Santiago, Chile;* [b]*Global Change Unit, Image Processing Laboratory, Universitat de Valencia, Valencia, Spain*

(*Received 30 December 2014; accepted 4 April 2015*)

This paper presents the Global Atmospheric Profiles derived from Reanalysis Information (GAPRI) database, which was designed for earth surface temperature retrieval. GAPRI is a comprehensive compilation of selected atmospheric vertical profiles at global scale which can be used for radiative transfer simulation in order to obtain generalized algorithms to estimate land surface temperature (LST). GAPRI includes information on geopotential height, atmospheric pressure, air temperature, and relative humidity derived from the European Centre for Medium-Range Weather Forecasts Re-Analysis data from year 2011. The atmospheric profiles are structured for 29 vertical levels and extracted from a global spatial grid of about 0.75° × 0.75° latitude–longitude with a temporal resolution of 6 hours. The selection method is based in the extraction of clear sky profiles over different atmospheric weather conditions such as tropical, mid-latitude summer, subarctic, and arctic, while also considering sea and land areas and day- and night-time conditions. The GAPRI database was validated by comparing land and sea surface temperature values derived from it to those obtained using other existing atmospheric profile databases and *in situ* measurements. Moreover, GAPRI was also compared to previous radiosonde atmospheric profiles using simulated split-window algorithms. Results show good agreement between GAPRI and previous atmospheric databases, thus demonstrating the potential of GAPRI for studies related to forward simulations in the thermal infrared range. GAPRI is a freely available database that can be modified according to the user's needs and local atmospheric conditions.

1. Introduction

Atmospheric gases such as water vapour, carbon dioxide, and ozone are important absorbers of energy at wavelengths in the atmospheric window located in the thermal infrared (TIR) range (8–14 μm). This absorption reduces the land-leaving radiance detected by sensors on board the Earth Observing (EO) satellites, and also contributes to the atmospheric emission detected by the sensor.

Atmospheric absorption and emission must be removed from the at-sensor registered TIR radiance in order to retrieve surface parameters such as land surface temperature (LST) and surface emissivity. This procedure is referred to in the literature as atmospheric correction or compensation, and it is a key factor in the accurate retrieval of land products from remote-sensing data. LST retrieval can be addressed from a direct inversion of the radiative transfer equation (RTE), which requires a detailed knowledge of the vertical structure of the atmosphere in order to account for atmospheric transmissivity and

*Corresponding author. Email: claudioduran@ug.uchile.cl

radiance (both up- and downwelling) (e.g. Jiménez-Muñoz et al. 2010); or by the simulation of comprehensive radiosounding data in order to obtain a generalized algorithm to estimate LST (Wan and Dozier 1996; Jiménez-Muñoz and Sobrino 2003; Tang et al. 2008; Jiménez-Muñoz and Sobrino 2008). In general terms, Split-Window (SW) algorithms have been conventionally used to retrieve LST from two TIR bands in the atmospheric window between 10 and 12 μm, which can be applied to a number of previous and current EO sensors (Jiménez-Muñoz and Sobrino 2008). Moreover, Single-Channel algorithms have also been developed to retrieve LST from one single TIR band, such as the Landsat series (Jiménez-Muñoz et al. 2009).

Most LST algorithms require the computation of certain coefficients obtained from simulations that use a number of atmospheric cases (and surface conditions). Once these coefficients are obtained, the LST algorithms can be applied in an operational way to generate LST products with minimum atmospheric input data (e.g. total atmospheric water vapour content). Several atmospheric profile databases have been developed for simulation purposes: the Thermodynamic Initial Guess Retrieval (TIGR) database (Aires et al. 2002; Chevallier et al. 2000), the radiosounding database for sea surface brightness temperature simulations (SAFREE) (François et al. 2002), and the Cloudless Land Atmosphere Radiosounding (CLAR) database (Galve et al. 2008). Despite the fact that TIGR data were updated in May 2010, other databases currently used in atmospheric correction do not include diverse atmospheric conditions or locations. For instance, the CLAR database does not include atmospheric profiles over sea, whereas the SAFREE database does not include atmospheric profiles over land, and TIGR2 is focused only on mid-latitudes. Moreover, these databases have fixed atmospheric profiles and do not include a clear night-/daytime differentiation, and thus the new database described below can fulfil these needs and offer an alternative for use in earth surface temperature retrieval.

In this article we present the Global Atmospheric Profiles derived from Reanalysis Information (GAPRI) database, which includes 8324 atmospheric profiles. Each individual profile is characterized by its geographical coordinates and acquisition characteristics (land/sea and day/night). The GAPRI database is supplied in Moderate Resolution Atmospheric Transmission (MODTRAN) code format (Berk et al. 1999) for simulation purposes.

2. Dataset

2.1. *ERA-Interim products*

The European Centre for Medium-Range Weather Forecasts Re-Analysis (ERA-Interim) products were used to generate the GAPRI database. These products are generated by the European Centre for Medium-Range Weather Forecasts (ECMWF) and have been available since 1979 to the present day. The ECMWF Integrated Forecast System (IFS Cy31r2) was used for the ERA-Interim product (Dee 2005; Uppala et al. 2008; Dee and Uppala 2009; Dee et al. 2011). ERA-Interim products present a wide range of environmental parameters at the global scale characterizing the surface, atmospheric levels, and potential vorticity at different time scales such as forecast, daily, or monthly means. A summarized description of ERA-Interim reanalysis products can be found in Gao, Bernhardt, and Schulz (2012). Even though other reanalyses can be used, such as the reanalysis from National Centers for Environmental Prediction and National Center for Atmospheric Research (NCEP-NCAR) (Kalnay et al. 1996; Kistler et al. 2001) or the Modern Era Retrospective-Analysis for Research and Applications from the Global Modeling and Assimilation Office (Rienecker et al. 2011), ERA-Interim has demonstrated its usefulness in remote-sensing applications

aimed at retrieving LST (Jiménez-Muñoz, Sobrino, Mattar, et al. 2014). Furthermore, partial comparisons between ERA-Interim and the MERRA database have been carried out for several parameters, demonstrating good agreement between both (Wang and Zeng 2012; Naud, Booth, and Del Genio 2014; Boilley and Wald 2015).

In this work, the 2011 global ERA-Interim air temperature, geopotential height, and relative humidity data set at 0.75° × 0.75° spatial resolution every 6 hours corresponding to 00.00, 06.00, 12.00, and 18.00 Coordinated Universal Time (UTC) were used. The year 2011 was selected following the El Niño Southern Oscillation index criteria where the period 2011–2012 was a weak Niña phase. The atmospheric parameters for that year were extracted at different isobaric levels provided by ERA-Interim from the low troposphere to the low stratosphere, and defined as: 1000, 975, 950, 925, 900, 875, 850, 825, 800, 775, 750, 700, 650, 600, 550, 500, 450, 400, 350, 300, 250, 225, 200, 175, 150, 125, 100, 50, and 20 hPa.

2.2. *Validation data*

In order to validate the GAPRI database, LST and sea surface temperature (SST) data provided by Advanced Very High Resolution Radiometer (AVHRR), Advanced Along-Track Scanning Radiometer (AATSR), and Moderate Resolution Imaging Spectroradiometer (MODIS) sensors were used in this work to perform the validation of earth surface temperature retrieved using the GAPRI database. Additionally, atmospheric databases such as TIGR (all versions – TIGR61, TIGR1761, and TIGR2311), the standard atmosphere of MODTRAN (STD66), and SAFREE were also used here to compare GAPRI to the surface temperature retrieved from these databases.

3. GAPRI database and validation

3.1. *Profile selection criteria*

Due to the large amount of ERA-Interim data, different selection criteria were adopted in order to construct a robust database capable of representing global atmospheric conditions with a moderate number of atmospheric profiles. These selection criteria are based on the selection of spatial location (land/sea), precipitable water content, and temporality.

3.2. *Spatial distribution*

In order to extract atmospheric profiles at the global scale over different locations, various ERA-Interim parameters such as air temperature, relative humidity, and geopotential height were compiled in global grid. These pixels were divided into ‘sea’ and ‘land’ (Figure 1) using a boolean land–sea mask product provided by ERA-Interim. Following this, the atmospheric variables (geopotential height, air temperature, and relative humidity) were extracted and structured into 29 atmospheric mandatory levels. This number of atmospheric levels is based on each of the ERA-Interim pressure levels from 1000 to 20 hPa where the maximum concentration of water vapour is mainly located. Despite the fact that we can include the maximum number of 34 vertical levels allowed in MODTRAN, the stratospheric levels (100–1 hPa) provided by ERA-Interim did not reveal any significant water vapour concentration relevant for TIR down- or upwelling irradiance in earth surface temperature retrieval. After the selection of this profile, a cloud filter was applied to select atmospheric profiles under clear sky conditions. This cloud filter is based on the maximum relative humidity of each level, so that ‘clear sky’ profiles were selected

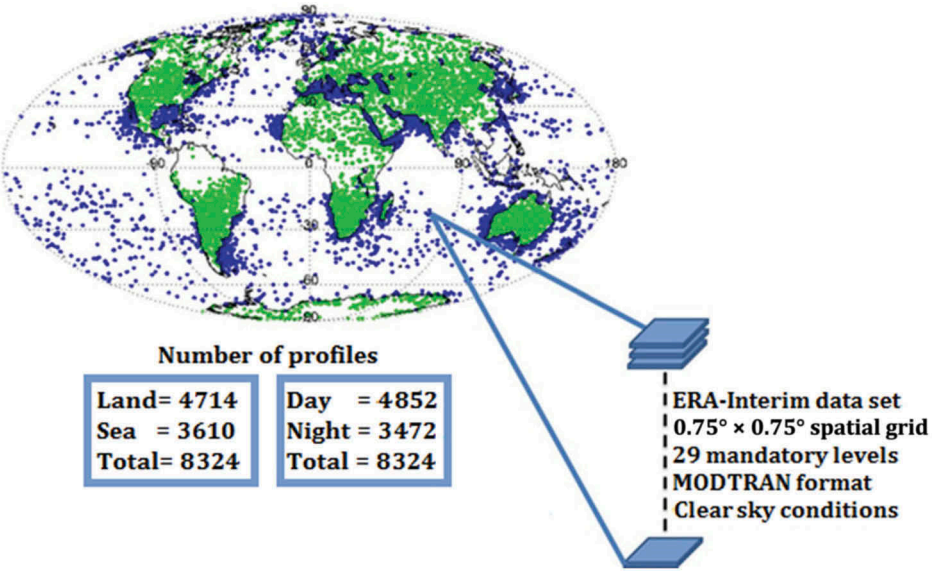

Figure 1. Location of atmospheric profiles extracted from ERA-Interim reanalysis to generate the GAPRI database. Green and blue points indicate profiles extracted over 'land' and 'sea'.

when relative humidity values were lower than 80% at each level. A similar criterion was used in Wang, Rossow, and Zhang (2000) using radiosonde data. Despite the fact that the cloud filter was successfully applied to radiosonde data, in numerical weather prediction the results may present some bias when performing comparison to *in situ* measurements or sounder profiles derived from satellites (Boilley and Wald 2015; Schreier et al. 2014). After application of the cloud filter, the total number of atmospheric profiles was reduced to 8324 (4714 over land and 3610 over sea).

3.3. *Precipitable water distribution*

The integrated water vapour column (defined as precipitable water (PW)) is a key atmospheric parameter in the TIR region, since water vapour is the most relevant absorbing gas in this thermal window region (Mattar et al. 2010). Therefore, it is reasonable to classify the different atmospheric profiles according to well-distributed values of this parameter. In the case of GAPRI, PW (in mm) was estimated from vertical integration of the specific humidity (q_v; in g kg^{-1}), which in turn was calculated from the saturation vapour pressure (e_s; in hPa):

$$e_s = 611\left(10^{\left(\frac{17.27T}{237.3+T}\right)}\right), \tag{1}$$

$$q_v = 0.622\frac{e_s(\mathrm{RH})}{100p}, \tag{2}$$

$$\mathrm{PW} = 0.01\int_{P_Z}^{P_0} q_v \mathrm{d}p \approx 0.01\sum \overline{q_v}\Delta p, \tag{3}$$

where T is the air temperature (°C), RH is the relative humidity (%), p is the atmospheric pressure (hPa) at each atmospheric layer, P_0 and P_Z correspond to lower and upper atmospheric pressure layers, respectively, and dp is a differential of atmospheric pressure. GAPRI vertical profiles were classified into five PW intervals: 0–10, 10–20, 20–30, 30–40, and 40–60 mm. The total number of vertical profiles for each PW class was equivalent and the atmospheric profile was randomly selected in order to be classified into one of these PW classes. Once the PW classes had been allocated a proportional number of vertical profiles, the PW selection criteria finished and the classification into day/night, land/sea, and atmospheric MODTRAN type begun.

3.4. Day/night classification

GAPRI atmospheric profiles were also classified into 'day' and 'night' acquisitions. This classification was performed by comparing the local solar time to the sunrise and sunset hours, using a set of equations that describe the solar time corrections and the position of the Sun relative to earth's surface according to Iqbal (1983). This day/night classification of the atmospheric profiles is related to the difference in LST retrievals when using one single PW value for daytime rather than the PW value close to the overpass of the satellite. The day/time separation criterion is detailed as follows.

3.4.1. Solar time and UTC

Solar time is a means of measuring time that is dependent on the rotation and translation of the earth. The length of the solar day varies throughout the year because it is affected by the tilt of earth's axis and the Earth–Sun distance. Thus, local and UTC time system measurements show a discrepancy with solar time that can fluctuate between –16 and +16 min. To calculate the true solar time (T_s), the time equation (Equation (4)) can be used (Spencer 1982), which corrects this time difference. Furthermore, the equation of time correction (T_c) (Equation (5)) includes the gap between local time (T_L) and UTC time (T_{utc}):

$$\mathrm{EoT} = 229.18(C_1 + C_2\cos(\gamma) - C_3\sin(\gamma) - C_4\cos(2\gamma) - C_5\sin(\gamma)), \tag{4}$$

$$T_c = 4(\lambda - 15(\Delta\mathrm{UTC})) + (\mathrm{EoT}), \tag{5}$$

where EoT is the equation of time, γ is the angular day in radians (Equation (6)) that depends on the day of the year (j), ΔUTC is the discrepancy between local and UTC time (Equation (7)), λ is the geographical longitude, $C_1 = 0.000075$, $C_2 = 0.001868$, $C_3 = 0.032077$, $C_4 = 0.014615$, and $C_5 = 0.04089$.

$$\gamma = \frac{\pi}{180}(j - 1). \tag{6}$$

$$\Delta\mathrm{GMT} = T_L - T_{utc}. \tag{7}$$

The true solar time can be calculated using Equation (8), which includes the equation of time correction and local time:

$$T_s = T_L + \frac{T_c}{60}. \tag{8}$$

Inserting Equations (4)–(7) into Equation (8), it is possible to simplify the expression of true solar time (Equation (9)):

$$T_s = T_{utc} + \frac{(4\lambda - (\mathrm{EoT}))}{60}. \tag{9}$$

3.4.2. Sunrise and sunset times and day/night classification

To estimate sunrise and sunset times, it is necessary to calculate the respective sunrise and sunset angles (Equations (10) and (11)):

$$w_{sr} = +a\cos(-\tan(\varphi)\tan(\delta)), \tag{10}$$

$$w_{ss} = -a\cos(-\tan(\varphi)\tan(\delta)), \tag{11}$$

where φ is the geographical latitude and δ is the sun's declination (Equation (12)). The parameters w_{sr} and w_{ss} are the sunrise and sunset angles, which have positive and negative values, respectively.

$$\delta = \frac{180}{\pi}(C_6 - C_7\cos(\gamma) + C_8\sin(\gamma) - C_9\cos(2\gamma) + C_{10}\sin(2\gamma) - C_{11}\cos(3\gamma) + C_{12}\sin(3\gamma)), \tag{12}$$

where γ is angular day in radians (Equation (6)), $C_6 = 0.006918$, $C_7 = 0.399912$, $C_8 = 0.070257$, $C_9 = 0.006758$, $C_{10} = 0.000907$, $C_{11} = 0.002697$, and $C_{12} = 0.00148$. To calculate sunrise and sunset times, Equations (13) and (14) can be used:

$$T_{sr} = 12 - \frac{w_{sr}}{15}, \tag{13}$$

$$T_{ss} = 12 - \frac{w_{ss}}{15}, \tag{14}$$

where T_{sr} and T_{ss} are the sunrise and sunset times, respectively. If $T_{sr} < T_s < T_{ss}$ then the corresponding profile will be assigned to day class, otherwise if $T_{sr} > T_s > T_{ss}$ it will be night class.

3.5. GAPRI database format

GAPRI database is presented in MODTRAN format. This radiative transfer code is widely used for the atmospheric correction of remotely sensed imagery (Berk et al. 2006; Anderson et al. 2009). The conversion of atmospheric profiles to MODTRAN radiative transfer code format is basically to standardize GAPRI into one standard format widely known in the remote-sensing atmospheric correction process. MODTRAN allows the input of up to 34 vertical levels, including meteorological parameters such as air temperature, relative humidity, dew point temperature, mixing ration, and geopotential height,

among others. Moreover, it includes six standard atmospheric profiles representative of different climatic conditions (tropical, mid-latitude summer, mid-latitude winter, subarctic summer, subarctic winter, and US standard atmosphere). This atmospheric model changes according to time and latitude, so the GAPRI atmospheric profiles were classified following the MODTRAN atmospheric model scheme. In order to complement the GAPRI atmospheric profiles, MODTRAN atmospheric models are also used to add atmospheric gases to the GAPRI profiles.

GAPRI profiles were converted to MODTRAN format ready for execution in thermal radiance mode with multiple scattering (16 streams), and with surface emissivity equal to one. Geopotential height (km), air temperature (K), and relative humidity (%) for each layer were extracted from the ERA-Interim product, whereas the remaining atmospheric constituents were retrieved from default values included in the MODTRAN standard atmospheres dependent on the location of the atmospheric profiles. Nevertheless, users can change the GAPRI format to adapt its input to other codes or MODTRAN options.

3.6. *Validation of GAPRI database*

In order to validate the GAPRI database, a comparison of simulated SW algorithms based on several surface emissivity values was performed between GAPRI, TIGR, and STD databases. Previous studies have demonstrated the application of GAPRI to SW coefficients retrieved for Landat-8 and geostationary data (Jiménez-Muñoz, Sobrino, Skokovic, et al. 2014; Jiménez-Muñoz, Sobrino, Mattar, et al. 2014b). Here, the performance of the GAPRI database for LST algorithm development was compared to other atmospheric profiles databases. For this purpose, we used the SW algorithm and low-resolution sensors employed by Jiménez-Muñoz and Sobrino (2008), such as AVHRR, AATSR, MODIS, Spinning Enhanced Visible and Infrared Imager (SEVIRI), and Geostationary Operational Environmental Satellite Imager (GOES). In this case, SW coefficients were obtained from forward simulations using the GAPRI database, whereas the algorithm was tested from simulated data extracted from various TIGR databases (TIGR-61, TIGR-1761, and TIGR-2311) and one database constructed from MODTRAN standard atmospheric profiles (STD-66), as described by Jiménez-Muñoz et al. (2009). For the simulation of LST, the surface temperature was assumed equivalent to the first temperature in the given atmospheric profile and the emissivity was obtained for each sensor band by using an average of 108 emissivity spectra extracted from the Aster spectral library (ASL). Moreover, GAPRI was also validated in LST retrieval using a compilation of satellite and *in situ* data in the framework of different initiatives:

(1) NOAA/AVHRR and European Remote Sensing Satellite 2 (ERS2) / Along-Track Scanning Radiometer 2 (ATSR2) data acquired over various Australian sites (Prata 1994);
(2) NOAA/AVHRR acquired in central Canada within the framework of the BOReal forest Ecosystem Study (BOREAS) (Sellers et al. 1995);
(3) TERRA/MODIS data acquired over a rice field in Spain (Coll, Wan, and Galve 2009).

The LST results were also compared to LST retrievals estimated from the TIGR database. Furthermore, since the GAPRI database can also be used for SST, an algorithm developed with the GAPRI-sea and SAFREE databases was also validated using NOAA/AVHRR data extracted from the Medspiration match-up database (Ruescas et al. 2011).

4. Results

4.1. Statistical description

Table 1 shows the number of atmospheric profiles for the different combinations of land/sea, day/night, standard atmosphere, and PW distribution. GAPRI covers almost all possible combinations between atmosphere type and PW values, except for some unrealistic cases such as subarctic atmospheres with high PW content. Most of the profiles are assigned to mid-latitude summer and tropical conditions, followed by subarctic summer and mid-latitude winter examples. The number of vertical profiles over land is in reasonable proportion to the number of vertical profiles over sea (57% and 43%, respectively), although the locations of the sea profiles are mainly distributed near continental coasts (Figure 1). In regard to PW classes, the number of vertical profiles included in each is also equally distributed (around 20% for each class), as well as the distribution between 'day' and 'night' values (58% and 42%, respectively). Further information about the distribution of the GAPRI profiles is provided in Figures 2 and 3, which show the histogram of the atmospheric profiles *versus* the PW content in terms of both day/night (Figure 2) and land/sea (Figure 3). These results also show a robust distribution of the different atmospheric profiles included in the GAPRI database.

Figure 4 plots the different atmospheric profiles over selected pixels for different regions of the world: Pacific, Indian, and Atlantic oceans, the Mediterranean Sea, the Sahara desert, Southern France, Amazon basin, and Eastern Russia. The thermal amplitude in the first atmospheric layers is noticeable over sea locations to 500 hPa. In regard to land, the differences are only evidenced in the Sahara desert, which revealed the highest air temperature on the first layers to 650 hPa. On the other hand, relative humidity revealed a marked difference for land and sea locations.

4.2. Validation of GAPRI

The results for LST simulation using GAPRI and other atmospheric databases are presented in Table 2. The mean difference between the GAPRI-derived algorithm and the other databases is near to 0 K and the standard deviation (1-sigma) is typically below 0.7 K, which demonstrates good performance of the GAPRI database, at least in comparison to other atmospheric profiles databases accepted by the scientific community. In most cases, comparisons to GAPRI are similar and the greatest differences in sigma were obtained for TIRG2311 and GOES13. Despite the fact that these results are derived from simulations of LST, it appears that GAPRI can be used as a potential atmospheric database with similar errors to those obtained when using TIGR databases for several TIR low-spatial resolution sensors.

On the other hand, validation of the GAPRI database using *in situ* LST is presented in Table 3. This table shows the bias, σ, and root mean square error (RMSE) when comparing *in situ* LST and that derived from NOAA, AATSR, and MODIS. The lowest RMSE was obtained when using GAPRI for the entire databases. Nevertheless, these results are similar to those obtained from other databases, because on average the improvement in RMSE shown by GAPRI is 0.11 K over the entire database. Using all NOAA data comparisons, GAPRI RMSE is the lowest above the entire atmospheric database, although no statistical differences exist with regard to the remainder of the atmospheric database ($p < 0.05$). In the case of SST (Table 4), the GAPRI database shows similar results to the SAFREE database, with a RMSE of about 0.1 K between both databases.

Table 1. Number of GAPRI atmospheric profiles for different combinations in terms of location (land/sea), time (day/night), assigned standard atmosphere (A1 = tropical; A2 = mid-latitude summer; A3 = mid-latitude winter; A4 = subarctic summer; A5 = subarctic winter), and precipitable water content (W1 = 0–10 cm; W2 = 10–20 cm; W3 = 20–30 cm; W4 = 30–40 cm; W5 = 40–60 cm).

	Land												Sea											
	Day						Night						Day						Night						
	A1	A2	A3	A4	A5	Total	A1	A2	A3	A4	A5	Total	A1	A2	A3	A4	A5	Total	A1	A2	A3	A4	A5	Total	Total
W1	10	68	180	158	13	429	7	57	215	131	32	442	63	30	95	87	28	303	70	25	120	84	62	361	1535
W2	86	257	64	150	1	558	62	175	18	127	0	382	203	118	21	68	11	421	156	90	6	68	4	324	1685
W3	177	160	62	161	0	560	137	137	11	91	0	376	94	133	95	115	0	437	99	73	11	75	0	258	1631
W4	245	194	4	108	0	551	181	156	0	59	0	396	169	175	0	112	0	456	110	77	0	74	0	261	1664
W5	288	285	0	34	0	607	170	224	0	19	0	413	342	184	0	4	0	530	143	114	0	2	0	259	1809
Total	806	964	310	611	14	2705	557	749	244	427	32	2009	871	640	211	386	39	2147	578	379	137	303	66	1463	8324

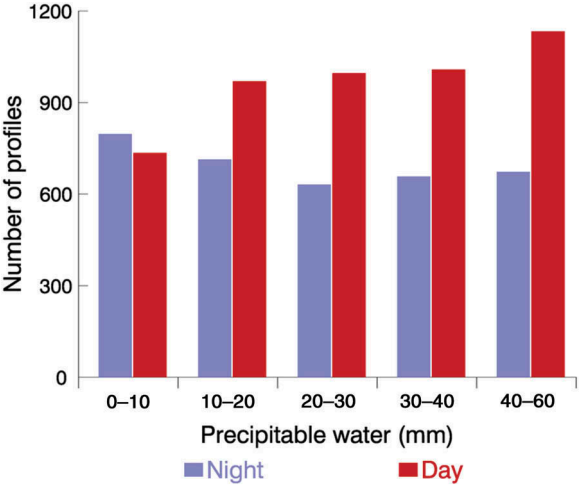

Figure 2. Number of vertical profiles according to the precipitable water class and daytime (red) and night-time (blue).

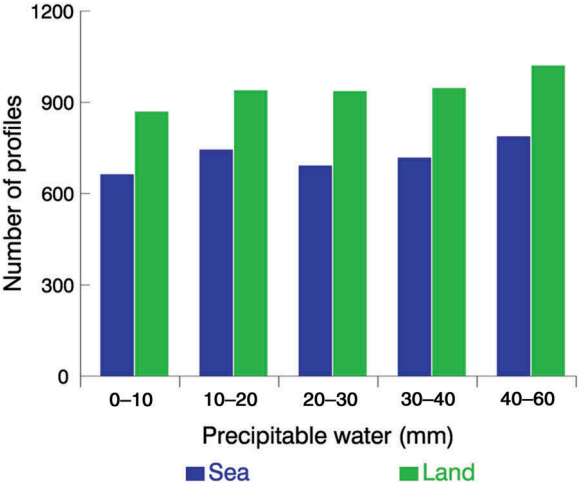

Figure 3. Number of vertical profiles according to the precipitable water class sea and land distribution.

5. Discussion and conclusions

Procedures based on radiative transfer simulations (e.g. forward simulations from different surface and atmospheric input data to reproduce radiance at the sensor level) are essential for algorithm development. Most thermal remote-sensing applications deal with the retrieval of LST, so algorithm development within this framework remains a topic of interest. In this sense, the availability of global reanalysis products provides a strong alternative to infrared soundings on board satellites or systematic launching of radiosonde (only available over particular areas). This option was previously explored for the atmospheric correction of the Landsat TIR band (Barsi, Barker, and Schott 2003; Barsi et al. 2005),

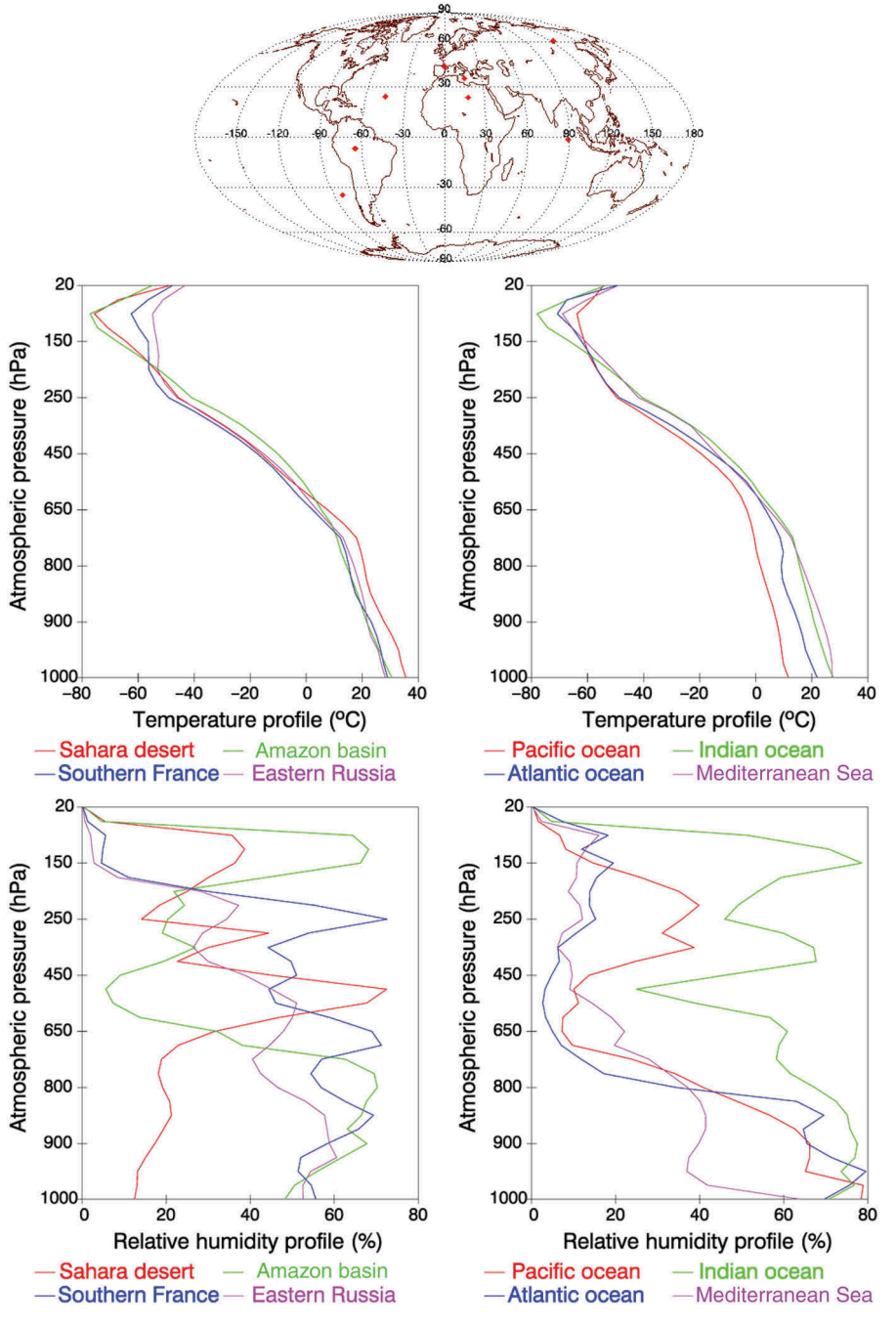

Figure 4. Comparison of different GAPRI profiles for selected pixels (top, red points) over land (left column) and over sea (right column).

and for atmospheric correction of different sensors using the modified atmospheric profiles from reanalysis information (MAPRI) database (Jiménez-Muñoz et al. 2010), a precursor of the current GAPRI database presented in this article.

Table 2. Validation of a split-window algorithm simulated for land surface temperature (LST) retrieval for different sensors.

Satellite sensor	Database	N	Bias ± σ (K)
Envisat-AATSR	TIGR61	6588	−0.1 ± 0.5
Envisat-AATSR	TIGR1761	190188	0.1 ± 0.3
Envisat-AATSR	TIGR2311	249588	0.2 ± 0.6
Envisat-AATSR	STD66	7128	0.0 ± 0.3
Terra-MODIS	TIGR61	6588	−0.1 ± 0.4
Terra-MODIS	TIGR1761	190188	0.2 ± 0.4
Terra-MODIS	TIGR2311	249588	0.2 ± 0.6
Terra-MODIS	STD66	7128	−0.2 ± 0.4
METOP-AVHRR3	TIGR61	6588	0.0 ± 0.5
METOP-AVHRR3	TIGR1761	190188	0.2 ± 0.3
METOP-AVHRR3	TIGR2311	249588	0.2 ± 0.6
METOP-AVHRR3	STD66	7128	0.0 ± 0.3
GOES13-IMG	TIGR61	6588	−0.3 ± 1.1
GOES13-IMG	TIGR1761	190188	0.0 ± 0.7
GOES13-IMG	TIGR2311	249588	0.0 ± 1.2
GOES13-IMG	STD66	7128	−0.2 ± 0.7
MSG2-SEVIRI	TIGR61	6588	−0.1 ± 0.5
MSG2-SEVIRI	TIGR1761	190188	0.2 ± 0.3
MSG2-SEVIRI	TIGR2311	249588	0.2 ± 0.6
MSG2-SEVIRI	STD66	7128	0.0 ± 0.3

Notes: Split-window coefficients were obtained from the GAPRI database, whereas the algorithm was tested from simulated data extracted from existing databases (TIGR61, TIGR1761, TIGR2311, and STD66). N refers to the number of test cases (number of atmospheric profiles multiplied by the 108 surface emissivities), and bias refers to the mean difference between LST obtained from GAPRI-derived coefficients and that included in other databases. Standard deviation of the difference (σ) is also given.

The atmospheric databases used for thermal infrared correction (TIGR or SAFREE) were rigorously elaborated by selecting radiosondes launched from either mainland or island sites. GAPRI is the first compilation of an ERA-Interim atmospheric profile presenting various vertical situations in different parts of the world (ocean, lakes, or continental areas) following the cloudless sky selection criteria. The main advantages of the GAPRI database are the complete location description of the different atmospheric profiles, as well as the date and time when they were selected, covering both land and sea, which in turn allows the creation of GAPRI-land or GAPRI-sea data sets. This is basically more suitable to the development of an SW algorithm focusing on one specific sensor operating at predetermined day- or night-time hours. On the other hand, the GAPRI database provides information about different MODTRAN atmospheric models and PW concentrations, thus allowing the user to select defined vertical profiles that reveal the most appropriate situation for its specific applications. For instance, the mid-latitude summer location can be adapted for specific PW concentrations, or locations in the tropical forest can also be used to select the profiles accounting for the highest PW concentrations for a given day- or night-time. Another feature of GAPRI is that atmospheric profiles are converted to MODTRAN format to allow a direct execution of the database in this radiative transfer code. It is also important to note that GAPRI was constructed from an automatic selection implemented in an operational mode, which means that other configuration options can be chosen and adapted to the user's requirements.

The results from the present study show that GAPRI presents a good agreement with TIGR and SAFREE databases, although its capabilities are dependent on the spatial

Table 3. Comparison between GAPRI and other atmospheric databases and *in situ* land surface temperature (K) derived from various low-spatial resolution sensors.

		GAPRI			TIGR61			TIGR1761			TIGR-2311			STD-66		
Sensor	Number of profiles	Bias (K)	σ (K)	RMSE (K)	Bias (K)	σ (K)	RMSE (K)	Bias (K)	σ (K)	RMSE (K)	Bias (K)	σ (K)	RMSE (K)	Bias (K)	σ (K)	RMSE (K)
NOAA7	110	0.85	1.48	1.70	1.10	1.51	1.87	0.86	1.48	1.71	1.03	1.49	1.81	1.10	1.50	1.86
NOAA9	110	1.28	1.49	1.96	1.62	1.56	2.24	1.25	1.49	1.95	1.49	1.51	2.12	1.57	1.53	2.19
NOAA11	301	−0.05	1.70	1.70	0.07	1.83	1.83	−0.16	1.75	1.76	−0.10	1.88	1.88	0.06	1.81	1.81
NOAA12	228	−0.30	1.62	1.65	−0.09	1.73	1.73	−0.24	1.70	1.71	−0.22	1.80	1.82	−0.07	1.73	1.73
NOAA14	110	0.27	1.48	1.51	0.53	1.47	1.57	0.39	1.48	1.53	0.50	1.48	1.56	0.55	1.47	1.57
ATSR2	36	−0.54	1.77	1.85	−0.70	1.79	1.92	−0.81	1.76	1.94	−0.79	1.89	2.05	−0.66	1.78	1.90
MODIS	23	−0.49	0.52	0.71	−0.45	0.55	0.71	−0.44	0.52	0.69	−0.39	0.55	0.67	−0.14	0.55	0.57
All NOAA	859	0.21	1.69	1.70	0.42	1.79	1.84	0.20	1.72	1.74	0.29	1.82	1.85	0.42	1.77	1.82
All data	918	0.16	1.68	1.69	0.35	1.78	1.82	0.15	1.72	1.72	0.24	1.82	1.83	0.36	1.76	1.80

Note: Bias, σ, and root mean square error (RMSE) for NOAA and the entire database are also shown.

Table 4. Comparison between GAPRI and SAFREE databases to *in situ* sea surface temperature (K) derived from various low-spatial resolution sensors.

		GAPRI			SAFREE		
Sensor	Number of profiles	Bias (K)	σ (K)	RMSE (K)	Bias (K)	σ (K)	RMSE (K)
NOAA14	14223	−0.80	1.51	1.71	−0.60	1.49	1.61

Note: Bias, σ, and root mean square error (RMSE) are also shown.

resolution of ERA-Interim reanalysis. Moreover, the detection of clouds may be impacted by the coarse spatial resolution, added to the rough cloud filter based on the relative humidity used in this study, which requires a simple approximation to establish whether the vertical profile is evidence of a potential concentration of water vapour attributed to clouds or not. However, the intercomparison between GAPRI and other well-established databases provided satisfactory results, which demonstrates the utility of this new database. Finally, a web-based interface will be developed in forthcoming work to facilitate downloading of the GAPRI database and also to compute radiative transfer simulation. Meanwhile, readers interested in using the current GAPRI version (or other modifications on-demand) can directly contact the authors.

Acknowledgements

The authors wish to thank the ECWMF for delivering the ERA-Interim data used in this work.

Disclosure statement

No potential conflict of interest was reported by the authors.

Funding

This work was partially funded by the project Fondecyt-Initial [CONICYT/ref 11130359] and the Ministerio de Economía y Competitividad of Spain [CEOS-Spain, AYA2011-29334-C02-01].

References

Aires, F., A. Chédin, N. A. Scott, and W. B. Rossow. 2002. "A Regularized Neural Net Approach for Retrieval of Atmospheric and Surface Temperatures with the IASI Instruments." *Journal of Applied Meteorology and Climatology* 41 (2): 144–159. doi:10.1175/1520-0450(2002)041<0144:ARNNAF>2.0.CO;2.

Anderson, G. P., A. Berk, P. K. Acharya, L. S. Bernstein, S. M. Adler-Golden, J. Lee, and L. Muratov. 2009. Reformulated atmospheric band model method for modeling atmospheric propagation at arbitrarily fine spectral resolution and expanded capabilities. U.S. Patent 7593835, filed September 22.

Barsi, J., J. Barker, and J. Schott. 2003. "An Atmospheric Correction Parameter Calculator for a Single Thermal Band Earth-Sensing Instrument." Paper presented at the International Geoscience and Remote Sensing Symposium, Toulouse, July 21–25.

Barsi, J., J. Schott, F. Palluconi, and S. J. Hook. 2005. "Validation of a Web-Based Atmospheric Correction Tool for Single Thermal Band Instruments." *Proceedings of SPIE* 5882: 0E.

Berk, A., G. P. Anderson, P. K. Acharya, L. S. Bernstein, L. Muratov, J. Lee, and M. Fox, et al. 2006. "MODTRAN 5: 2006 Update." *Proceedings of SPIE* 6233: 1F.

Berk, A., G. P. Anderson, P. K. Acharya, J. H. Chetwynd, L. S. Bernstein, E. P. Shettle, M. W. Matthew, and J. H. Adler-Golden. 1999. *MODTRAN4 User's Manual*. Hanscom AFB, MA: Air Force Research Laboratory.

Boilley, A., and L. Wald. 2015. "Comparison between Meteorological Re-Analyses from Era-Interim and MERRA and Measurements of Daily Solar Irradiation at Surface." *Renewable Energy* 75: 135–143. doi:10.1016/j.renene.2014.09.042.

Chevallier, F., A. Chédin, F. Cheruy, and J.-J. Morcrette. 2000. "Tigr-Like Atmospheric-Profile Databases for Accurate Radiative-Flux Computation." *Quarterly Journal of the Royal Meteorological Society* 126 (563): 777–785. doi:10.1002/qj.v126:563.

Coll, C., Z. Wan, and J. M. Galve. 2009. "Temperature-Based and Radiance-Based Validations of the V5 MODIS Land Surface Temperature Product." *Journal of Geophysical Research* 114: D20102. doi:10.1029/2009JD012038.

Dee, D. P. 2005. "Bias and Data Assimilation." *Quarterly Journal of the Royal Meteorological Society* 131 (613): 3323–3343. doi:10.1256/qj.05.137.

Dee, D. P., and S. Uppala. 2009. "Variational Bias Correction of Satellite Radiance Data in the Era-Interim Reanalysis." *Quarterly Journal of the Royal Meteorological Society* 135 (644): 1830–1841. doi:10.1002/qj.v135:644.

Dee, D. P., S. M. Uppala, A. J. Simmons, P. Berrisford, P. Poli, S. Kobayashi, and U. Andrae, et al. 2011. "The Era-Interim Reanalysis: Configuration and Performance of the Data Assimilation System." *Quarterly Journal of the Royal Meteorological Society* 137 (656): 553–597. doi:10.1002/qj.828.

François, C., A. Brisson, L. Le Borgne, and A. Marsouin. 2002. "Definition of a Radiosounding Database for Sea Surface Brightness Temperature Simulations. Application to Sea Surface Temperature Retrieval Algorithm Determination." *Remote Sensing of Environment* 81 (2–3): 309–326. doi:10.1016/S0034-4257(02)00008-1.

Galve, J. M., C. Coll, V. Caselles, and E. Valor. 2008. "An Atmospheric Radiosounding Database for Generating Land Surface Temperature Algorithms." *IEEE Transactions on Geoscience and Remote Sensing* 46 (5): 1547–1557. doi:10.1109/TGRS.2008.916084.

Gao, L., M. Bernhardt, and K. Schulz. 2012. "Elevation Correction of ERA-Interim Temperature Data in Complex Terrain." *Hydrology and Earth System Sciences* 16: 4661–4673. doi:10.5194/hess-16-4661-2012.

Iqbal, M., ed. 1983. "Extraterrestrial Solar Irradiation." Chap. 4 in *An Introduction to Solar Radiation*. Ontario: Academic Press.

Jiménez-Muñoz, J. C., J. Cristóbal, J. A. Sobrino, G. Sòria, M. Ninyerola, and X. Pons. 2009. "Revision of the Single-Channel Algorithm for Land Surface Temperature Retrieval from Landsat Thermal-Infrared Data." *IEEE Transactions on Geoscience and Remote Sensing* 47 (1): 339–349. doi:10.1109/TGRS.2008.2007125.

Jiménez-Muñoz, J. C., and J. A. Sobrino. 2003. "A Generalized Single-Channel Method for Retrieving Land Surface Temperature from Remote Sensing Data." *Journal of Geophysical Research* 108 (D22): 4688. doi:10.1029/2003JD003480.

Jiménez-Muñoz, J. C., and J. A. Sobrino. 2008. "Split-Window Coefficients for Land Surface Temperature Retrieval from Low-Resolution Thermal Infrared Sensors." *IEEE Geoscience and Remote Sensing Letters* 5 (4): 806–809. doi:10.1109/LGRS.2008.2001636.

Jiménez-Muñoz, J. C., J. A. Sobrino, C. Mattar, and B. Franch. 2010. "Atmospheric Correction of Optical Imagery from MODIS and Reanalysis Atmospheric Products." *Remote Sensing of Environment* 114 (10): 2195–2210. doi:10.1016/j.rse.2010.04.022.

Jiménez-Muñoz, J. C., J. A. Sobrino, C. Mattar, and G. Hulley. 2014. "Temperature and Emissivity Separation from MSG/SEVIRI Data." *IEEE Transactions on Geoscience and Remote Sensing* 52 (9): 5937–5951. doi:10.1109/TGRS.2013.2293791.

Jiménez-Muñoz, J. C., J. A. Sobrino, D. Skokovic, C. Mattar, and J. Cristóbal. 2014. "Land Surface Temperature Retrieval Methods from Landsat-8 Thermal Infrared Sensor Data." *IEEE Geoscience and Remote Sensing Letters* 11 (10): 1840–1843. doi:10.1109/LGRS.2014.2312032.

Kalnay, E., M. Kanamitsu, R. Kistler, W. Collins, D. Deaven, L. Gandin, and M. Iredell, et al. 1996. "The NCEP/NCAR 40-Year Reanalysis Project." *Bulletin of the American Meteorological Society* 77 (3): 437–471. doi:10.1175/1520-0477(1996)077<0437:TNYRP>2.0.CO;2.

Kistler, R., W. Collins, S. Saha, G. White, J. Woollen, E. Kalnay, and M. Chelliah, et al. 2001. "The NCEP–NCAR 50–Year Reanalysis: Monthly Means CD–ROM and Documentation." *Bulletin of*

the American Meteorological Society 82 (2): 247–267. doi:10.1175/1520-0477(2001)082<0247:TNNYRM>2.3.CO;2.

Mattar, C., J. A. Sobrino, Y. Julien, and L. Morales. 2010. "Trends in Column Integrated Water Vapour over Europe from 1973 to 2003." *International Journal of Climatology* 31 (2): 1497–1757.

Naud, C. M., J. F. Booth, and A. D. Del Genio. 2014. "Evaluation of ERA-Interim and MERRA Cloudiness in the Southern Ocean." *Journal of Climate* 27 (5): 2109–2124. doi:10.1175/JCLI-D-13-00432.1.

Prata, A. J. 1994. "Land Surface Temperatures Derived from the Advanced Very High Resolution Radiometer and the Along-Track Scanning Radiometer." *Journal of Geophysical Research* 99 (D9): 13025–13058.

Rienecker, M. M., M. J. Suarez, R. Gelaro, R. Todling, J. Bacmeister, E. Liu, and M. G. Bosilovich, et al. 2011. "MERRA: NASA's Modern-Era Retrospective Analysis for Research and Applications." *Journal of Climate* 24: 3624–3648. doi:10.1175/JCLI-D-11-00015.1.

Ruescas, A. B., M. Arbelo, J. A. Sobrino, and C. Mattar. 2011. "Examining the Effects of Dust Aerosol Son Satellite Sea Surface Temperatures in the Mediterranean Sea Using the Medspiration Matchup Database." *Journal of Atmospheric and Oceanic Technology* 28 (5): 684–697. doi:10.1175/2010JTECHA1450.1.

Schreier, M. M., B. H. Kahn, K. Sušelj, J. Karlsson, S. C. Oul, Q. Yue, and S. L. Nasiri. 2014. "Atmospheric Parameters in a Subtropical Cloud Regime Transition Derived by AIRS and MODIS: Observed Statistical Variability Compared to ERA-Interim." *Atmospheric Chemistry and Physics*: 14: 3573–3587. doi:10.5194/acp-14-3573-2014.

Sellers, P., F. Hall, K. J. Ranson, H. Margolis, B. Kelly, D. Baldocchi, and G. den Hartog, et al. 1995. "The Boreal Ecosystem Atmosphere Study (BOREAS): An Overview and Early Results from the 1994 Field Year." *Bulletin of the American Meteorological Society* 76 (9): 1549–1577. doi:10.1175/1520-0477(1995)076<1549:TBESAO>2.0.CO;2.

Spencer, J. W.. 1982. "A Comparison of Methods for Estimating Hourly Diffuse Solar Radiation from Global Solar Radiation." *Solar Energy* 29 (1): 19–32. doi:10.1016/0038-092X(82)90277-8.

Tang, B. H., Y. Bi, Z.-L. Li, and J. Xia. 2008. "Generalized Split-Window Algorithm for Estimate of Land Surface Temperature from Chinese Geostationary Fengyun Meteorological Satellite (FY-2C) Data." *Sensors* 8 (2): 933–951. doi:10.3390/s8020933.

Uppala, S., D. P. Dee, S. Kobayashi, P. Berrisford, and A. Simmons. 2008. "Towards a Climate Data Assimilation System: Status Update of ERA-Interim." *ECMWF Newsletter* 115: 12–18. http://old.ecmwf.int/publications/newsletters/pdf/115.pdf.

Wan, Z. M., and J. Dozier. 1996. "A Generalized Split-Window Algorithm for Retrieving Land-Surface Temperature from Space." *IEEE Transactions on Geoscience and Remote Sensing* 34 (4): 892–905. doi:10.1109/36.508406.

Wang, A., and X. Zeng. 2012. "Evaluation of Multireanalysis Products with In Situ Observations over the Tibetan Plateau." *Journal of Geophysical Research* 117: D5.

Wang, J., W. Rossow, and Y. Zhang. 2000. "Cloud Vertical Structure and Its Variations from a 20-Yr Global Rawinsonde Dataset." *Journal of Climate* 13 (17): 3041–3056. doi:10.1175/1520-0442(2000)013<3041:CVSAIV>2.0.CO;2.